

# **Production of high-resolution remote sensing images for navigation information infrastructures**

Wang Zhijun<sup>a,\*</sup>, Djemel Ziou<sup>a</sup>, Costas Armenakis<sup>b</sup>

<sup>a</sup> Dept of mathematics and informatics, University of Sherbrooke, Sherbrooke, Quebec, Canada J1K 2R1

<sup>b</sup> Natural Resources Canada, Center for Topographic Information (CTI), Geomatics Canada, 615 Booth Str., Ottawa, Ontario, Canada K1A 0E9

## **Abstract**

This paper introduces the image fusion approach of Multi-Resolution Analysis-based Intensity Modulation (MRAIM) to produce high-resolution multi-spectral images from high-resolution panchromatic image and low-resolution multi-spectral images for navigation information infrastructure. The mathematical model of image fusion is derived based on the principle of remote sensing image formation. It shows that the pixel values of the high-resolution multi-spectral images are determined by the pixel values of an approximation of the high-resolution panchromatic image at the resolution level of low-resolution multi-spectral images. The M-band wavelet theory and the à trous algorithm are then used to compute the pixel values of the approximation of the high-resolution panchromatic image at the resolution level of the low-resolution multi-spectral images. In order to evaluate the MRAIM approach, an experiment has been carried out based on the IKONOS 1m panchromatic image and 4m multi-spectral images. The result demonstrates that MRAIM image fusion approach gives promising fusion results and it can be used to produce the high-resolution remote sensing images required for navigation information infrastructures.

*Keywords:* Image fusion; MRAIM algorithm; Navigation information infrastructure

## **1. Introduction**

The recent advancements of information technologies has had a great impact on the vehicle technology (Auto21, 2003). There is a need to construct an integrated Navigation Information Infrastructure (NII) to supply the most relevant information that the driver and on-board systems need to improve navigation and guidance, driving safety, and enhanced accessibility to location-based service. Up-to-date geo-spatial information is the main information of NII. Remote sensing provides the opportunity to frequently collect the up-to-date geo-spatial information of interested areas. It is advantageous to include multi-resolution remote sensing images in the construction of NII to deal with the various scale-related aspects. The first commercial satellite IKONOS, launched on Sept. 24, 1999, provides 1m resolution panchromatic images and 4 m multi-spectral images. This permits objects of approximately one meter in length to be identified on the earth's surface using a satellite in outer space. Image fusion techniques are used to combine information from multi-sensor images to enhance image information and improve information extraction capability. Through image fusion, it is expected that 1m resolution multi-spectral images can be produced and used in the construction of NII.

The algorithms of fusing high-resolution panchromatic image with low-resolution multi-spectral image have evolved from traditional methods such as RGB, IHS, PCA,

---

\* Corresponding author: Email: [wangz@dmi.usherb.ca](mailto:wangz@dmi.usherb.ca); Tel. +1-819-8218000-2855; Fax: +1-819-8218200

pyramid-base methods to nowadays wavelet-based methods (Yocky, 1995; Liu, 2000; Núñez, et al., 1999; Li, 1999; Pohl, et al. 1998; Wald, et al., 1997; Wald, 1999; Wang, 2000; Wang, et al., 2000). Wavelet transform is an intermediate representation between Fourier and spatial representation and provides good localization properties in both spatial and Fourier domain, therefore wavelet-based fusion methods can improve the spatial resolution while preserve the spectral characteristics at a maximum degree (Yocky, 1996). Currently used wavelet-based image fusion methods are mostly based on two fast computation algorithms: Mallat algorithm and à trous algorithm (Shensa, 1992). Those methods have some shortcomings. Due to down sampling, Mallat algorithm introduces **aliasing** in the fused image. The à trous algorithm cannot ensure a smoothing transition of amplitude from the low-frequency part of multi-spectral image to high-frequency part of high resolution image. Histogram matching must be applied before fusion and each channel is added by the same high-frequency part of high-resolution image during fusion process, thus the saturation of the image is degraded. The MRAIM approach (Wang, 2000; Wang et al., 2000) is designed to overcome the above-mentioned problems. It can be used to solve the fusion problem with different integer ratios (**other than 2**) between the resolutions of panchromatic image and multi-spectral images.

In this paper, the MRAIM algorithm is applied to produce 1m high-resolution multi-spectral images from IKONOS 1m high-resolution panchromatic image and 4m low-resolution multi-spectral images. The performance of this algorithm is evaluated in terms of improving the spatial resolution while preserving the spectral characteristics.

## 2. Image fusion algorithm of MRAIM

In this section, the image fusion approach of Multi-Resolution Analysis based Intensity Modulation (MRAIM) is introduced (Wang, 2000; Wang et al., 2000). It takes into consideration the principle of remote sensing image formation (Liu, 2000), M-band wavelet theory (Steffen, et al., 1993) and à trous algorithm (Shensa, 1992)

The physical principle of image formation is based on the simplified solar radiation model and the land surface reflectance model. The energy of solar radiation, which approximates that of a 5900K black body, is mainly concentrated in the visible and near-infrared spectral region (0.4-2.4 $\mu$ m). When incident on terrain, this solar radiation with irradiance  $E(\lambda)$  is partially and selectively reflected, transmitted and absorbed by the terrain materials. The reflected solar energy can be recorded by reflective panchromatic and spectral band sensors to produce panchromatic image and multi-spectral images. Different materials have characteristic spectral reflection and absorption features and therefore can be mapped in terms of different Digital Number (DN) in these images. Based on a simplified radiation transfer model, where also DN=radiance, the DN value of a daytime optical image of reflective spectral band is mainly determined by three factors: the given incident solar radiation  $M_s$ , the spectral reflectance  $\rho(\lambda)$  of the land surface and the angle  $\gamma$  between the land surface and the incident solar radiation (Liu, 2000):

$$DN(\lambda) = \rho(\lambda)M_s \sin \gamma \quad (1)$$

For a specific spectral band of the remote sensing image under certain solar illumination

condition, the DN is mainly controlled by topography factor  $\gamma$  (sun elevation). A slope facing the sun receives more solar radiation and therefore has higher irradiance and reflectance than a shaded slope. As a result, the illuminated slope appears bright in both reflective spectral and panchromatic images.

The general mathematical model for image fusion can be derived from Eq. (1). Let us consider a unit surface corresponding to a pixel of the higher resolution image  $I_{high}$  of band  $\lambda$ . It corresponds to the sub-pixel of a low-resolution image  $I_{low}$  of same band and same area. For the reason of pixel-level image fusion,  $I_{low}$  is up-sampled to  $SI_{low}$  at the pixel size as  $I_{high}$ . Let us denote  $DN_{high}(\lambda)$  as a DN value of the pixel in  $I_{high}$  and  $DN_{low}(\lambda)$  the DN value of the corresponding pixel in  $SI_{low}$ . We assume the high-resolution and low-resolution images of band  $\lambda$  are taken at the same time. It means that the incident solar radiation  $M_s$  and spectral reflectance  $\rho(\lambda)$  are identical to each other. So we have:

$$DN_{high}(\lambda) = \rho(\lambda)M_s \sin(\gamma_{high}) \quad (2)$$

$$DN_{low}(\lambda) = \rho(\lambda)M_s \sin(\gamma_{low}) \quad (3)$$

$\gamma_{high}$  is the angle between incident solar radiation and the corresponding unit surface. Since  $DN_{low}(\lambda)$  in  $SI_{low}$  was computed from the corresponding unit surface of  $I_{low}$  in which the pixel covers larger land surface area than a unit surface of  $I_{high}$ , the angle  $\gamma_{low}$  refers to the angle between the incident radiation and the larger land surface area and it is usually not same to  $\gamma_{high}$ . Dividing Eq. (2) by Eq. (3), gives:

$$\frac{DN_{high}(\lambda)}{DN_{low}(\lambda)} = \frac{\sin(\gamma_{high})}{\sin(\gamma_{low})} \quad (4)$$

Eq. (4) demonstrates that the ratio between  $DN_{high}(\lambda)$  and  $DN_{low}(\lambda)$  is controlled by the topography factor  $\gamma$  and is independent of the spectral characteristics of the terrain objects. Let us assume that there are panchromatic and multi-spectral sensors observe the same terrain area and that there is no topographic change during the acquisition dates of panchromatic and the multi-spectral images. If  $\lambda_{pan}$  represents a panchromatic band and  $\lambda_{MS}$  a multi-spectral band, then based on Eq. (4) and for  $\lambda=\lambda_{pan}$  and  $\lambda=\lambda_{ms}$ , we have:

$$\frac{DN_{high}(\lambda_{pan})}{DN_{low}(\lambda_{pan})} = \frac{DN_{high}(\lambda_{MS})}{DN_{low}(\lambda_{MS})} \quad (5)$$

Manipulating Eq (5), leads to equivalent expression:

$$DN_{high}(\lambda_{MS}) = DN_{low}(\lambda_{MS}) + \alpha \cdot w \quad (6)$$

where  $w = DN_{high}(\lambda_{pan}) - DN_{low}(\lambda_{pan})$  (sometimes it is also called wavelet plane (Wang, 2000))

and  $\alpha = \frac{DN_{low}(\lambda_{MS})}{DN_{low}(\lambda_{pan})}$ .  $w$  represents the detail information between the high and low resolution

images and  $\alpha$  is the modulation coefficient for the detail information. When the panchromatic image and the multi-spectral images are acquired by the same platform,  $\alpha = \frac{\rho(\lambda_{MS})}{\rho(\lambda_{pan})}$ . For

visual purpose, 3 bands multi-spectral images are usually used to form a colour image in application. Then Eq. (6) becomes:

$$\begin{bmatrix} DN_{high}(\lambda_{MS1}) \\ DN_{high}(\lambda_{MS2}) \\ DN_{high}(\lambda_{MS3}) \end{bmatrix} = \begin{bmatrix} DN_{low}(\lambda_{MS1}) \\ DN_{low}(\lambda_{MS2}) \\ DN_{low}(\lambda_{MS3}) \end{bmatrix} + w \cdot \begin{bmatrix} \alpha_1 \\ \alpha_2 \\ \alpha_3 \end{bmatrix} \quad (7)$$

$DN_{high}(\lambda_{pan})$  and  $DN_{low}(\lambda_{MSi}), \{i = 1,2,3\}$  are known,  $DN_{low}(\lambda_{pan})$  and

$DN_{high}(\lambda_{MSi}), \{i = 1,2,3\}$  are unknown. As long as  $DN_{low}(\lambda_{pan})$  is approximated,

$DN_{high}(\lambda_{MSi}), \{i = 1,2,3\}$  can be solved for. This shows that the pixel values of the

high-resolution multi-spectral images are determined by the pixel values of the approximation of the high-resolution panchromatic image at the resolution level of low-resolution multi-spectral image. So the performance of the fusion process is also determined by the performance of the way to estimate  $DN_{low}(\lambda_{pan})$ .

From the M-band wavelet theory (Steffen, et al., 1993; Chan, et al., 1998; Wisutmethangoon et al., 1999; Nguyen and Koilpillai, 1996), we learned that the multi-resolution analysis decomposition method is the tool to decompose signals to their approximation and detail information. M-band wavelet transform is different from the most popular used dyadic wavelet transform in the respect that M-band wavelet transform decomposes the frequency domain into M-channels while dyadic wavelet transform into 2 channels. So M-band wavelet transform can be used to compute the approximation at resolution M (M is a arbitrary positive integer larger than 0) while dyadic wavelet transform is limited to the resolution of  $2^r (r \in I)$ . The key problem to realize this approach is to construct K-regularity M-band scale filters. K-regularity

is equivalent to saying that all polynomials of degree (K-1) are contained in approximation. This coupled with the compact support characteristic of the scaling filters implies that K-regularity scaling filters can be used to capture local polynomial behaviour. Steffen et al. (1993) introduced the formula for K-regularity M-band scaling filter  $H_0(z)$  in the Z transform of the analysis and synthesis process of the M-band scaling, which is just as in the 2-band case Daubechies' construction. For  $K = 2$ , the minimal phase and maximal phase solution for arbitrary  $M$  is given by the following formula:

$$H_0(z) = \left[ \frac{1 + z^{-1} + \dots + z^{-(M-1)}}{M} \right]^2 (q_{(0)} + q_{(1)}z^{-1}) \quad (8)$$

Where,

$$q_{(0)} = \frac{\sqrt{M}}{2} \left[ 1 \pm \sqrt{\frac{2M^2 + 1}{3}} \right] \text{ and } q_{(1)} = \frac{\sqrt{M}}{2} \left[ 1 \mp \sqrt{\frac{2M^2 + 1}{3}} \right] \quad (9)$$

Upon the construction of the scale filters, the à trous algorithm (Shensa, 1992) is applied to compute the panchromatic image at the low-resolution level by filtering. Initially, the à trous algorithm is defined for the case  $M=2$  (i.e., dyadic wavelet transform). We extended it to a more general case, that is M-band wavelet transform. Given an image  $p_1$  at resolution level 1, the approximation  $p_M$  at resolution level M can be computed by low-pass filtering the image  $p_1$ .

The reconstruction formula can be written as:

$$p_1 = p_M + w \quad (10)$$

Once the approximation image  $p_M$  is ready, it can be used in Eq. (7) to compute the fused image. This method is named Multi-Resolution Analysis-based Intensity Modulation (MRAIM) (Wang, 2000).

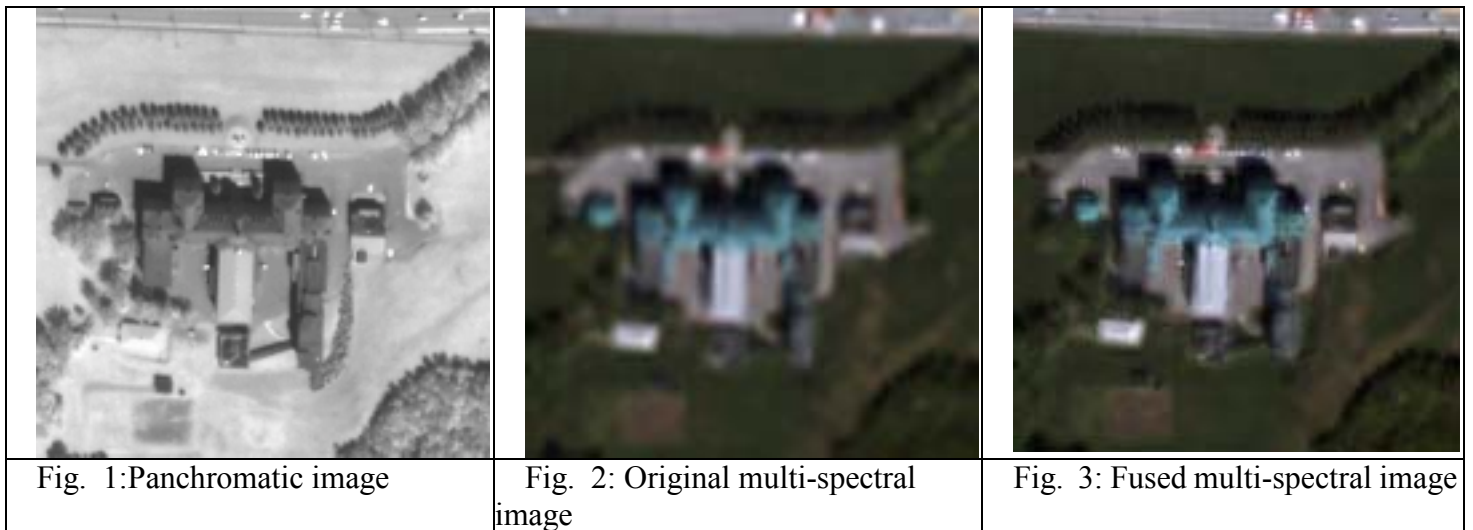
### 3. Experiment and discussion

In order to evaluate the performance of MRAIM algorithm, IKONOS-2 panchromatic and multi-spectral images of part of Sherbrooke city area, Quebec, Canada, have been used to study the performance of MRAIM algorithm. Since IKONOS consists of four-band multi-spectral images, three for visible and one from Near Infra Red (NIR) part of the spectrum, only the three visible bands are selected in order to visual inspect the fusion process. The size of the panchromatic dataset is 256\*256 and multi-spectral images is 64\*64. The study area is composed of various features such as cars, church built-up area, isolated trees, meadow and street-light posts etc. The size of those features ranges from less than 1m up to 100m.

Since the spatial resolution of panchromatic image is 1m and the multi-spectral images is 4m, a 4-band à trous filter driven by the square of K-regularity 4-band scale filter  $H_o(n)$ , where  $K=2$ , has been applied in our case. The fusion procedure is described as follows:

- (1) Linear stretch panchromatic image (see Fig. 1).
- (2) Linear stretch multi-spectral images.
- (3) Registration of multi-spectral images to panchromatic image with less than 0.5 pixel RMS and up-sampled to 1m pixel size (see Fig. 2).
- (4) Decomposition of the original panchromatic image into its approximation image and wavelet plane using the à trous algorithm.
- (5) Fusion of the panchromatic image and multi-spectral images using the MRAIM algorithm (see Fig. 3).

Fig. 1 shows the panchromatic image, Fig. 2 shows the original 4 m resolution multi-spectral images but up-sampled into 1 m pixel size, and Fig. 3 shows the fused result, that is the 1m multi-spectral images.

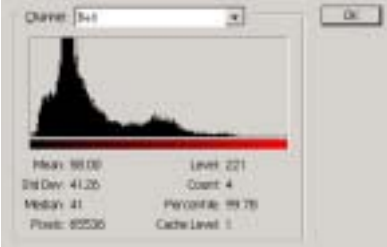
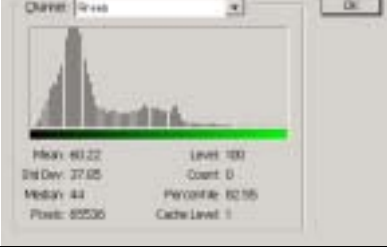
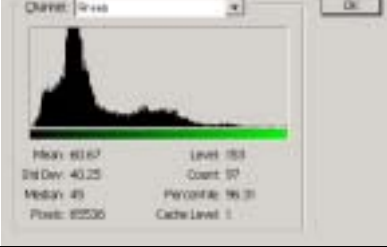
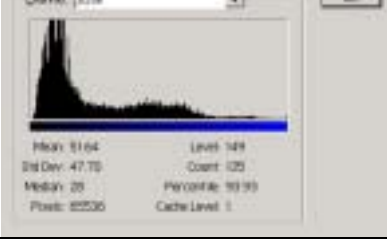


The criteria for the assessment of the fusion result depend on the application (Wald, et al., 1997). In this paper, we try to improve the spatial resolution while preserve the spectral characteristics unchanged. This can be understood from another point of view, that is, how to simulate the high-resolution multi-spectral image from the available low-resolution multi-spectral images and high-resolution panchromatic image. In this case, the fusion process can be evaluated in terms of spatial and spectral quality, respectively. The assessment of spatial quality can be evaluated by comparing the panchromatic image and the fused image to see whether the structures of the objects in panchromatic image are injected into the multi-spectral images and the assessment of spectral quality can be checked by comparing the fused image with the original multi-spectral image to see whether the radiometry of the two images is as identical as possible. But for the time being, there are no effective ways to evaluate the fusion result both qualitatively and quantitatively. Visual inspection is still the most common method to evaluate the fusion result qualitatively. In additional, several quantitative indexes such as mean, median, standard deviation, correlation coefficient, etc., can be also used to assess the

fusion result quantitatively. In this paper, we use visual inspection to evaluate the fusion results qualitatively and use statistical parameters mean, median, standard deviation, and correlation coefficient to evaluate the degree of similarity between the original images and the fused images.

The assessment of the spatial quality is carried out by visually comparing the panchromatic image (Fig. 1) and the fused image (Fig. 3). It was found that the objects in panchromatic image (Fig. 1), for example, cars, isolated trees and street-light posts, can be also identified in Fig. 3, indicating that the spatial information has been injected into the fused multi-spectral image. More detailed information can be identified in the fused image. For instance, the color of the cars can be discriminated in the fused image which otherwise is not possible to be identified in either panchromatic image or the original multi-spectral image.

Table 1: Statistical parameters of mean, standard deviation and median of the histogram of the RGB channels of original image and the fused image, and the correlation coefficients between the RGB channels of the original image and the fused image

Histogram of original images	Histogram of fused image	Correlation
 <p>Channel: Red  Mean: 57.69      Level: 112  Std Dev: 39.21      Count: 489  Median: 41      Percentile: 98.38  Pixels: 65536      Cache Level: 1</p>	 <p>Channel: Red  Mean: 59.00      Level: 221  Std Dev: 41.26      Count: 4  Median: 41      Percentile: 99.78  Pixels: 65536      Cache Level: 1</p>	0.9814
 <p>Channel: Green  Mean: 63.22      Level: 100  Std Dev: 37.05      Count: 0  Median: 44      Percentile: 92.98  Pixels: 65536      Cache Level: 1</p>	 <p>Channel: Green  Mean: 63.67      Level: 103  Std Dev: 40.25      Count: 97  Median: 45      Percentile: 96.31  Pixels: 65536      Cache Level: 1</p>	0.9800
 <p>Channel: Blue  Mean: 51.34      Level: 109  Std Dev: 45.39      Count: 0  Median: 29      Percentile: 91.83  Pixels: 65536      Cache Level: 1</p>	 <p>Channel: Blue  Mean: 51.64      Level: 149  Std Dev: 47.75      Count: 129  Median: 29      Percentile: 93.93  Pixels: 65536      Cache Level: 1</p>	0.9854

For the spectral quality assessment, it was also found visually that the color of the fused image looks very similar to the original multi-spectral image. In addition, the statistical parameters of the fusion result were compared with the original multi-spectral image and the correlation coefficients (between channels) were also computed. Table 1 presents the statistical parameters of mean, standard deviation and median of the histogram of the RGB channels of original image and the fused images as well as the correlation coefficients between the RGB channels of the original image and the fused image.

The difference in the mean and median values of the fused and the original images explains

the difference in the central tendency. It can be found from Table 1 that mean value and median value of the RGB channels of the original multi-spectral image are almost identical as in the fused image. The difference in standard deviation can globally represent the level of detailed information. The higher the standard deviation, the more detailed information. After the fusion process, the standard deviation of each channel of fused image is increased. This shows that more detailed information is included in the fused image and it is consistent with the visual inspection results. The correlation coefficients between the RGB channels of original multi-spectral image and the fused image resulted are 0.9814, 0.9800, and 0.9854, respectively. Since the correlation coefficient represents the degree of similarity, the value of the correlation coefficient is desirable to be as higher as possible, but it cannot reach to 1 which means that the fused image is the same with the original multi-spectral image and no spatial information from panchromatic image is added to the fused image. In this sense, it shows that the MRAIM algorithm results in a very higher similarity between original multi-spectral image and the fused images.

In the MRAIM approach, steps 1 and 2 are pre-processing procedures. The purpose of those steps is to improve the registration accuracy of step 3. They can be omitted and still give the same fused result in terms of linear stretch enhancement without the registration accuracy. Both from the statistical and the visual inspection point of view, the MRAIM image fusion algorithm can be used to fuse IKONOS remote sensing images and the fusion result is promising.

In our experiment, for simplicity reasons, only three channels of multi-spectral images have been selected. However, this approach is not limited to three channels, as it can be applied to any number of channels of multi-spectral images.

#### **4. Conclusion**

Imagery significantly contributes in the creation of vehicle NII either as one of the information spatial layers or for the updating of the geo-bases. Particularly, image fusion assists in the enhancement of feature detection, recognition and extraction. The MRAIM image fusion approach has been proposed to fuse high-resolution panchromatic image with multi-spectral low-resolution images to produce high-resolution multi-spectral images. It is based on the principle of image formation, M-band wavelet theory and à trous algorithm. It injects the high-frequency component of the panchromatic image into the re-sampled multi-spectral images. It was showed in this study that the MRAIM approach posses the capability of preserving spectral characteristics among multi-spectral images while improving the spatial resolution. It can be used to produce the high-resolution remote sensing images for navigation information infrastructure. Our experiment is based on IKONOS panchromatic image and multi-spectral images, but the concept can be also applied to other images, such as Landsat-7 panchromatic image (15m) and multi-spectral images (30m) by using 2-band à trous filter, and SPOT panchromatic image (10m) and Landsat multi-spectral images by using 3-band à trous filter.

#### **References**

- AUTO21. [http://www.auto21.ca/home\\_e.html](http://www.auto21.ca/home_e.html). accessed Jan. 12, 2003.  
Chan S.C., Luo Y., Ho K.L. , 1998. M-channel compactly supported biorthogonal

- cosine-modulated wavelet bases. IEEE Trans. on SP 46(4), 1142-1151.
- Li J., 1999. The theory, algorithms and practice of multi-sensor remote sensing image fusion. PhD thesis, Wuhan Technical University of Surveying and Mapping, Wuhan, P.R.China. (In Chinese)
- Liu J.G., 2000. Smoothing filter-based intensity modulation: a spectral preserve image fusion technique for improving spatial details. INT. J. Remote Sensing, 21(18), 3461-3472.
- Nguyen T.Q., Koilpillai R.D., 1996. The theory and design of arbitrary-length Cosine-modulated filter banks and wavelets, satisfying perfect reconstruction. IEEE Trans. on SP 44(3), 473-483.
- Núñez J., Otazn X., Fors O., Prades A., Palà, Romá Arbiol V., 1999. Image fusion with additive multi-resolution wavelet decomposition: Application to SPOT+Landsat images. J. Opt. Soc. Am. A 16(3), 467-473.
- Pohl C., **Gendern J. L. Van**, 1998. Multi-sensor image fusion in remote sensing: concepts, methods and applications. Int J Remote Sensing 19(5), 823-854.
- Shensa M.J., 1992. The discrete wavelet transform: wedding the à Trouns and Mallat algorithms. IEEE Trans. on SP 40(10), 2464-2482.
- Steffen P., Heller P. , . Gopinath R.A, . Burrus C.S., 1993. Theory of regular M-band wavelet Bases. <http://www.supelec-rennes.fr/ren/perso/jweiss/wavelets.html>. Wavelet Resources, accessed Jan. 12, 2003.
- Wald L., 1999. Some Terms of Reference in Data Fusion. IEEE Trans. On Geoscience and Remote Sensing 37(3), 1190-1193.
- Wald L., Ranchin T., Mangolini M., 1997. Fusion of satellite images of different spatial resolutions: assessing the quality of resulting images. Photogrammetric Engineering & Remote Sensing 63, 691-699.
- Wang Z., 2000, Wavelet Transform Based Multi-sensor Remote Sensing Image Fusion. PhD thesis, Wuhan University. Wuhan, P.R.China.
- WangZ., Li D., Li Q., 2000. A Introduction to Multi-resolution Based Grey Modulation Image Fusion Method. Proc. CPGIS'2000. 21-23 June, Monterey, USA.
- Wisutmethangoon Y, Nguyen T.Q., 1999. A method for design of Mth-band filters. IEEE Trans. on SP 47(6), 1669-1678.
- Yocky D.A, 1995. Image merging and data fusion by means of the discrete two-dimensional wavelet transform. J. Opt. Soc. Am A 12(9), 1834-1841.